

Potential Application of Particle Image Velocimetry To Sub-Sonic Open Circuit Wind Tunnel

Vishvendra Singh Tomar^{a,*}, Sahib Chawla^a, Shanu Sinha^a, Raj Kumar Singh^a, Arun Dhyani^b

^aDepartment of Mechanical Engineering, Delhi Technological University, New Delhi, India

^bDepartment of Electronics and Communication Engineering, Delhi Technological University, New Delhi, India

Article Info

Article history:

Received 29 December 2013

Received in revised form

10 January 2014

Accepted 20 January 2014

Available online 1 February 2014

Keywords

Particle Image Velocimetry

Sub-Sonic Open Circuit Wind Tunnel

Mach Number

Correlation Technique

Flow Measurement

Abstract

In this present work, Particle Image Velocimetry (PIV) as a flow visualization technique with vast potential is applied to determine the Flow Velocity Distribution around an object placed in the Test Chamber of a Sub-Sonic Open Circuit Wind Tunnel (SOWT) [Mach Number (M) = 0.15]. The two challenging tasks to accomplish during the development of instrumental set up are: 1. Electronic System Development for reducing the flash time so as to have a sharp image of the particle flow. 2. Seeding System Development by incorporating the air bubbles generators. Some details of PIV hardware, programmable PIV processor and software architecture are also discussed, emphasizing the practical benefits of various features. Further, to relax the PIV, filtered motion blurring technique has been utilized using Auto-Correlation.

1. Introduction

Particle Image Velocimetry (PIV) is the most recent entrant to the field of non-intrusive fluid flow measurement which provides instantaneous velocity fields and flow particles displacement pattern over global (2D or 3D) domains. It records the position over time of small tracer particles introduced into the flow to determine the local fluid velocity. Basically, It consists of an optically transparent test-section containing the flow seeded with tracer particles, an illuminating light source (laser), a recording medium (CCD camera) and a computer with suitable software to process the recorded images and extract the velocity information based on certain algorithms [1, 2], as shown in Fig. 1.

Hinsch [3] described, a measurement system to be labeled as (α, β, γ) , where $\alpha = 1, 2, 3$ indicating the number of velocity components measured, $\beta = 0, 1, 2, 3$ indicating the number of spatial dimensions of the measurement domain and $\gamma = 0, 1$ indicating instantaneous or continuous time recording, respectively. For 2D analysis, system can be referred $(2, 2, 0)$ and also, the majority of PIV systems in use

today belong to this category. For 3D analysis, systems are described as $(3, 2, 1)$ which provide 3D velocity data on planar domains and are becoming increasingly popular. Thus, PIV provides too much flexibility in measurements of a wide range of systems.

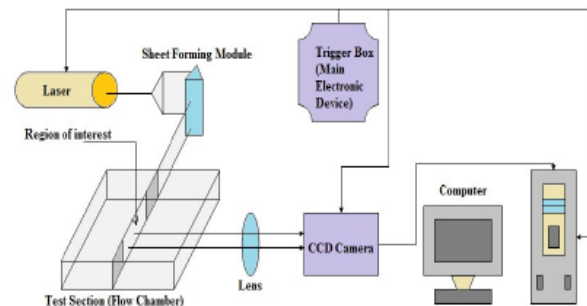


Fig. 1. A basic instrumental set up for PIV System

In today's world, Everyone's main focus is to save time, material and money which have compelled us to opt for the experimental testing on scale models, before the final product is to be shaped. The Wind Tunnel is one such platform, which provides us the appropriate desired environment conditions around

Corresponding Author,

E-mail address: vst.dtu@gmail.com

All rights reserved: <http://www.ijari.org>

The model scaled to the compatible dimensions. The Sub-Sonic Open Circuit Wind Tunnel can be described as the tunnel having flow velocity less than that of sound with both ends open to the ambient conditions, usually comes into role when the model is to be tested around flow velocity of 50m/s or 150 Km/hr (Fig. 2.) [4, 5]. The tunnel is supplied with a Test Chamber for flow visualization and proper monitoring but it has its own limitations ranging from accuracy to Macro-Level Measurements. Especially when flow visualization around a very small orifice or some Micro-Level portion is required, it is quite unsuitable. Thus, to enhance the flexibility of the tunnel, PIV can be used to visualize the flow in place of the Test Chamber, without any modification to rest of the tunnel.

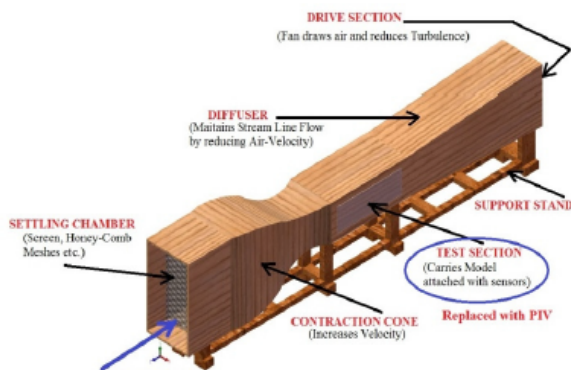


Fig. 2: A basic Isometric View of the complete model of SOWT developed using 3D Solid Modeling Program

Although the idea of application of PIV to the tunnel is quite alluring, but the real difficulty lies at: 1] As the lamps or the lasers have a flash time of the order of milliseconds, it is quite complicated to process the image and correlate the outcomes, Even more difficult at high turbulence flow. Ideal processing requires a time delay of at least some ten microseconds (μs) for a fluid speed of the order of some ten meter per second which is very smaller than the flash light decay. 2] In the tunnel, as there is flow of gases (which is not the usual case, like liquids), it is desirable to have a particle image of the same order of a pixel size, maybe of the order of 1 mm. So, the choice of the seeding particles restricts PIV's direct application to the tunnel. However with the latest technology embedded in various Electronics Circuits and Mechanical Devices, It has become possible to curb down the above limitations [6, 7]. The possible solutions are discussed in the next two sections.

2. Electronic Switch Circuit Using IGBT and SCR

There are two choices for practical implementation of switch used to turn off the lamp namely power MOSFET or IGBT, in this work IGBT is chosen to minimize the decay period. In this, the switching time is not too small but the current value is of the value of few hundred amperes which is to be turned off. IGBT has its own disadvantages too due to its large gate charge which provides it two main difficulties. The first difficulty is related to the beginning of the switch-off of the drain current directly depending on the gate-to-drain charge thus causing a delay in the shut off of the lamp with respect to trigger pulse. In fact the first part of the switch off process is the decrease of the gate voltage from its "HIGH" value to the "TRANSITION" one (Fig. 3.), by discharging the drain-to-gate charge. For reducing this time the gate current must be large, but also the "high" to "transition". It is usually good practice to have a large voltage difference to avoid staying in the intermediate stages and to dissipate power on the device. The solution to this problem is found using a powerful SCR as final driving device for the final IGBT. If C is the gate capacitance then a large resistor R is used in order to have a large value of RC so that gate voltage can be kept "HIGH". But it must be short enough to be able to relight the lamp for the next flash, while the gate is discharged via a small resistor by the SCR which is kept "FIRED" for such a time, to be sure that the deionization process of the lamp is finished and an "ON" transition of the IGBT will not restart the lamp. Therefore the trigger pulse that excites the lamp will also trigger a two stages mono-stable multi-vibrator, the first one generating the time delay for the flash duration, the second one the time for keeping "ON" the SCR. Of course, the power supply must be able to fully recharge the main capacitor before the next flash (Fig. 4 & 5).

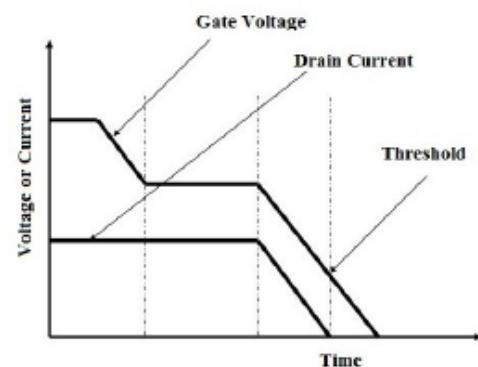


Fig. 3. Qualitative discharge process and different timing of the IGBT.

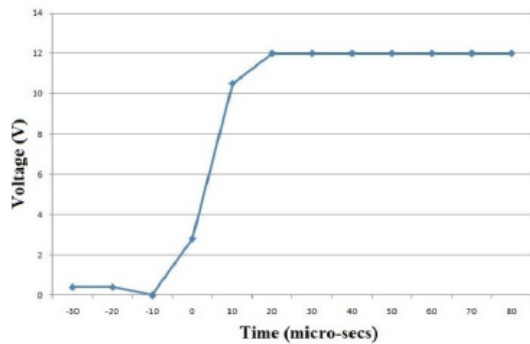


Fig. 4. Variation of IGBT collector voltage versus time.

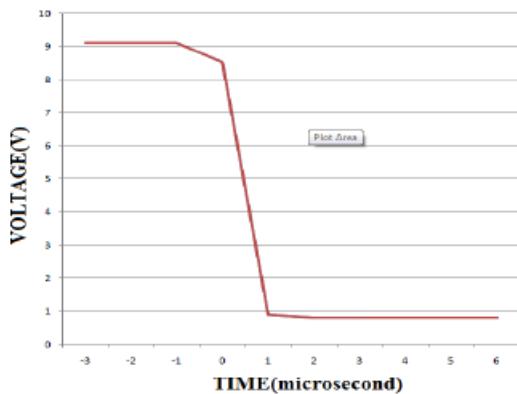


Fig. 5. Variation of IGBT gate voltage versus time.

3. Bubbles as Seeding Particles

In flow measurements where air is used as fluid, the application of soap bubbles were faced with many problems, mainly due to the difficulty of having a RAKE of bubble generators working simultaneously and due to the bubble inflation when subjected to increase the bubbles emission rate. A bubble generator consists of three concentric tubes: a] The inner one injects the filling gas, b] The medium one having high surface tension liquid (water and soap) form the liquid film of the bubble, c] The third one detaches the bubbles.

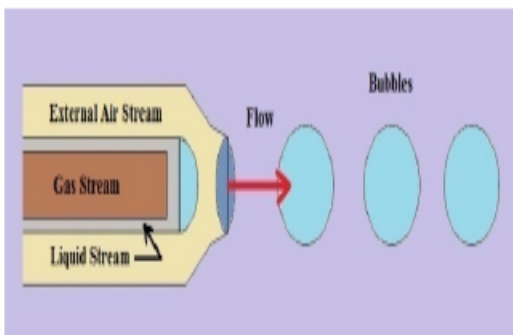


Fig. 6: Bubble generator ejecting bubbles, during air flow.

With the bubble generator described above (Fig. 6.), bubbles of a diameter almost equal to the liquid tube can be obtained, as first at a small rate. To have a much more uniform stream and a better bubble behavior a converging outer tube is added to the generator with addition of some percent of glycerin to the water-soap-mixture, providing the bubbles a lifetime of some ten seconds. Also, the liquid film of the bubbles is slightly fluorescent which causes the color dispersed by the bubbles to shift slightly toward the red increasing again the "noise" in the digitized image and requiring a further software improvement.

4. CCD Sensors as Recording Hardware and other Processing Hardware

PIV images may be recorded on a film or on CCD (Charge Coupled Device) cameras. The commonly available 8-bit $1\text{ k} \times 1\text{ k}$ CCD sensors can store only 1 M-byte per frame. These sensors allow the set-up processes to be accomplished in a few seconds. Digital PIV results can be viewed in almost real-time with high-speed on-board computational hardware dedicated towards computing correlations. These CCD sensors are far more light-sensitive than the film which allows them to perform the same experiment with a far less powerful laser, producing cost benefits and a safer working environment. They also provide a linear response to light intensity in contrast to the film which responds logarithmically and allow interrogation with smaller spots (in terms of pixels). Several vendors provide frame-grabbers to interface the CCD camera to the computer. The processing of PIV frames can also be performed efficiently on the PC, especially using dedicated array processing hardware. The basic requirement is that the FFT operation be performed extremely rapidly and the hardware must also support high-speed graphics to enable the visualization of the particle field, and the plotting of vector fields in almost real time [8-10].

5. PIV Relaxation Using Filtered Motion Blurring Technique

In this the start and end positions of the blurring image are filtered and the filtered image data is Auto-Correlated, which usually shows a peak similar to that of cross-correlation of PIV revealing the direction and value of displacement (Fig. 7.). The approach used in this paper applies simple kernel filters but compensates for the impact of the particle size on the measured velocity. This is achieved measuring its size based on the highlighted width of the particle.

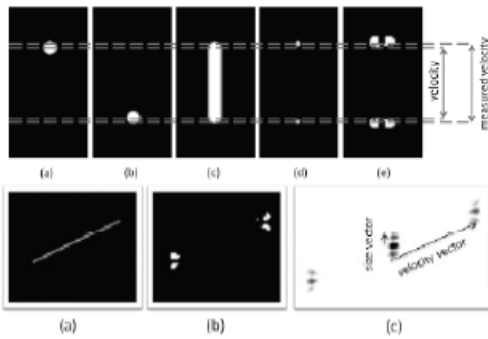


Fig. 7. Filtered Motion Technique, Using Particle Image's Intensity.

The filter results are achieved by applying Sobel filter kernels that are supplemented by a suppression factor s . The effect of the parameter s is to suppress the motion blur while maintaining the start and end position of the blurring (Fig. 8.).

$$F_{x^+} = \begin{pmatrix} 1 & 2 & \bar{s} & -2 & -1 \\ 4 & 8 & -s & -8 & -4 \\ 6 & 12 & 0 & -12 & -6 \\ 4 & 8 & -s & -8 & -4 \\ 1 & 2 & -s & -2 & -1 \end{pmatrix} \quad F_{x^-} = \begin{pmatrix} -1 & -2 & -\bar{s} & 2 & 1 \\ -4 & -8 & s & 8 & 4 \\ -6 & -12 & 0 & 12 & 6 \\ -4 & -8 & s & 8 & 4 \\ -1 & -2 & -s & 2 & -1 \end{pmatrix}$$

$$F_{y^+} = \begin{pmatrix} -1 & -4 & -6 & -4 & -1 \\ -2 & -8 & -12 & -8 & -2 \\ -s & -s & 0 & -s & -s \\ 2 & 8 & 12 & 8 & 2 \\ 1 & 4 & 6 & 4 & 1 \end{pmatrix} \quad F_{y^-} = \begin{pmatrix} 1 & 4 & 6 & 4 & 1 \\ -2 & -8 & -12 & -8 & -2 \\ -s & -s & 0 & -s & -s \\ -2 & -8 & -12 & -8 & -2 \\ -1 & -4 & -6 & -4 & -1 \end{pmatrix}$$

Input: I Image (N,M)
Output: \vec{v} : Velocity Vector ; \vec{s} : Size Vector
Data: I_x, I_y, I_{yx}, I_{xy} : Grayscale Image (N,M)
 B_{yx}, B_{xy}, R : Binary Image (N,M)
 C : Autocorrelation Matrix (M+N-1, M+N-1)
 P_1, P_2, P_3 : Point

References

[1] "Particle image velocimetry: a review", Fluid Loading and Instrumentation Centre, Heriot-Watt University, Edinburgh, Scotland
 [2] M Jahanmiri, "Particle Image Velocimetry: Fundamentals and its Applications," Division of Fluid Dynamics, Department of Applied Mechanics, Chalmers University of Technology, Goteborg, Sweden, 2011
 [3] K. D. Hinsch, Meas. Sci. Technol., 1995, 742–753
 [4] Types of Wind Tunnels, NASA Aeronautics and Space Administration, <http://www.grc.nasa.gov/WWW/k-12/airplane/tuntype.html>

```

1 begin
2    $I_x = (F_x^+ * I) + (F_x^- * I)$ 
3    $I_{yx} = (F_y^+ * I_x) + (F_y^- * I_x)$ 
4    $B_{yx} = \text{Binarize}(I_{yx}, 255 \rightarrow 1, 0 \dots 254 \rightarrow 0)$ 
5
6    $I_y = (F_y^+ * I) + (F_y^- * I)$ 
7    $I_{xy} = (F_x^+ * I_y) + (F_x^- * I_y)$ 
8    $B_{xy} = \text{Binarize}(I_{xy}, 255 \rightarrow 1, 0 \dots 254 \rightarrow 0)$ 
9
10   $R = B_{yx} \circ B_{xy}$  % Hadamard multiplication
11   $C = \text{Autocorrelation}(R)$ 
12   $P_1 = \text{argMax}_1(C)$ 
13   $P_2 = \text{argMax}_2(C)$ 
14   $P_3 = \text{argMax}_3(C)$ 
15
16  if  $|P_1 P_2| > |P_1 P_3|$  then
17     $\vec{v} = P_1 P_2$ ;  $\vec{s} = P_1 P_3$ 
18  else
19     $\vec{v} = P_1 P_3$ ;  $\vec{s} = P_1 P_2$ 
20  end
21 end
    
```

Fig. 8. Algorithm followed to calculate the velocity.

The results are invariant to the angle of the motion blurring. The vector with the highest norm is assumed to represent the velocity, the other is considered as size vector. For very thin motion blurring, a size vector may not be detected. In those particular cases, only the velocity vector is calculated and the width of the blurring is set to 1 pixel. Thus, the filtered motion technique can be applied to relax the PIV instrumentation [11-13].

6. Conclusion

The prospective appliance of PIV as a non-intrusive flow measurement technique with high degree of accuracy can be utilized to evaluate Velocity Distribution and Flow visualization in Wind tunnel. With optimum design of electronic & mechanical devices, the desired results can be obtained. Further, with inclusion of Latest Hardware and Software Techniques, It provides too much flexibility.

[5] "Science Buddies: How to Build a Subsonic Wind Tunnel" <http://www.sciencebuddies.org/science-fairprojects/wind-tunnel.toc.shtml>.
 [6] S. Deponle, S. Frmzctti, G. Cilbertini, S. MalaVaSi, "Tow-Colour Flash P.I.V. Technique for Relatively large Flow Fields". 8th International Conference on Laser Anemometry Advances 2nd Application, Rome, 6-8 September 1999
 [7] C. E. Towers, P. J. Bryanston-Cross, T. R. Judge, "Application of particle image velocimetry to large-scale transonic wind tunnels, "Optics dr Laser Technology, Vol. 23. No 5, pp. 289-295, 1991

- [8] L. Rockstroh, S. Wahl, S. Simon, R. Gadow, "Accuracy of 2d particle image velocimetry measurements in thermal spraying processes," in International Thermal Spray Conference, 2011
- [8] A. K. Prasad, R. J. Adrian, C. C. Landreth, P. W. Offutt, *Exp. Fluids*, 1992, 13, 105–116
- [9] A. Boillot, A. K. Prasad, *Exp. Fluids*, 1996, 21, 87–93
- [10] J. Westerweel, D. Dabiri, M. Gharib, *Exp. Fluids*, 1997, 23, 20–28
- [11] Tinne Tuytelaars, Krystian Mikolajczyk, "Local invariant feature detectors: a survey," *Foundations and Trends in Computer Graphics and Vision*, 3(3), pp. 177–280, 2008
- [12] L. Rockstroh, S. Wahl, Z. Wang, P. Werner, R. Gadow, S. Simon, "A technique to relax particle image velocimetry based on linear spatial filters," in European Signal Processing Conference, 2011
- [13] A. M. Lopez, F. Lumbreras, J. Serrat, J. J. Villanueva, "Evaluation of methods for ridge and valley detection," in *Pattern Analysis and Machine Intelligence*, 1999, 21, pp. 327–335